CERN-INTC-2023-055 / INTC-P-671
26/09/2023

EUROPEAN ORGANIZATION FOR NUCLEAR RESEARCH

Proposal for the ISOLDE and Neutron Time-of-Flight Committee

New measurement of the ^{146}Nd(n,γ) cross section at n_TOF-EAR2

September 26, 2023

J. Lerendegui-Marco[1], C. Domingo-Pardo[1], B. Gameiro[1], V. Babiano-Suárez[2], M. Bacak[3], J. Balibrea-Correa[1], F. Calviño[4], A. Casanovas[4], G. Cortés[4], S. Cristallo[5,6], U. Köster[7], I. Ladarescu[1], C. Lederer[8], M. Lugaro[9,10,11], N. Liu[12], E. Odusina[8], G. Rovira[13], B. Soós[9,10,11], N. Sosnin[8], B. Szányi[9,10,11], A. Tarifeño-Saldivia[1], D. Vescovi[5,6] and the n_TOF Collaboration[14]

[1] *Instituto de Física Corpuscular (CSIC - Universitat de València), Spain*
[2] *Universitat de València, Spain*
[3] *European Organization for Nuclear Research (CERN), Switzerland*
[4] *Universitat Politècnica de Catalunya, Spain*
[5] *INFN, Sezione di Perugia, Perugia, Italy*
[6] *INAF, Observatory of Abruzzo, Teramo, Italy*
[7] *Institut Laue-Langevin ILL, Grenoble, France*
[8] *School of Physics and Astronomy, University of Edinburgh, United Kingdom)*
[9] *Konkoly Observatory, Research Centre for Astronomy and Earth Sciences, Hungary*
[10] *CSFK, MTA Centre of Excellence, Hungary*
[11] *ELTE Eötvös Loránd University, Institute of Physics, Hungary*
[12] *Institute for Astrophysical Research, Boston University, USA*
[13] *Japan Atomic Energy Agency (JAEA), Tokai-Mura, Japan*
[14] *www.cern.ch/n_TOF*

Spokesperson: J. Lerendegui-Marco (jorge.lerendegui@ific.uv.es)
Technical coordinator: O. Aberle (oliver.aberle@cern.ch)

Abstract:

The abundance ratio of the Nd isotopes produced by the s-process in AGB stars is mostly controlled by the neutron cross sections of the Nd isotopes and can be constrained using measurements of SiC grains in meteorites. Several problems are present when comparing the SiC data with model predictions. One of the main issues is that the ^{146}Nd/^{144}Nd abundance ratio is clearly overpredicted and state-of-the-art s-process AGB calculations indicate that a 15% higher neutron-capture cross section of ^{146}Nd, in particular below 10 keV, would lead to a better agreement. With the aim of solving this present discrepancy,

we propose a new measurement of this cross section at the CERN n_TOF Facility. Combining the high-flux facility n_TOF-EAR2, a high sensitivity setup, and using a sample containing 80 mg of 98.7% pure ^{146}Nd, we aim to measure for the first time the resonance region up to 5 keV, thus allowing a consistent re-evaluation of the cross section focused mainly on the low stellar temperature range kT=8 keV.

Requested protons: 3.7×10^{18}.
Experimental Area: EAR2

1 Motivation

Stardust SiC grain measurements give the most precise observational data currently available on isotopic ratios produced by s-process nucleosynthesis (in fact, isotopic abundances cannot be derived using spectroscopic observations). Together with experimental cross sections, stardust data can yield the most sensitive constraint for stellar models. Focusing on Nd, the measured isotopic ratios of bulk samples of fine-grained silicon carbide (SiC) from meteorites exhibit some discrepancies when compared with recent model predictions for the envelope compositions of Asymptotic Giant Branch (AGB) stars of 2–3 $M_\odot$ and metallicity close to solar, the parent stars of the grains [1]. Also when using ^{146}Nd as representative of the total elemental abundance of Nd, there is a disagreement of a factor of 2 with its elemental abundance in SiC relative to all the other lanthanides of the REE group [2]. Nd isotopic ratios have been published both from bulk grains (i.e. collections of million of grains) by different experimental methods (TIMS, SIMS, ICP-MS) over the last decades [3, 4, 5], all of them showing consistent results for the ^{146}Nd/^{144}Nd abundance ratio. In general, a higher neutron-capture cross section of ^{146}Nd would lead to a better agreement between the SiC data and the stellar predictions [2, 5].
New s-process calculations have been carried out to evaluate the sensitivity of the predicted abundance ratios to the ^{146}Nd(n,γ) cross section [6], using the FUNS [7] and the MONASH [8] codes for AGB stars of 2–3 $M_\odot$ and solar metallicity Z=0.014. The results for the ^{146}Nd/^{144}Nd relative to the ^{150}Nd/^{144}Nd are shown in the left panel of Fig. 1. The experimental abundances are taken from one single SiC grain reported by Liu [9] and the average of bulk data measured by Richter et al. [1].
The lines in the left panel of Fig. 1 correspond to different ^{146}Nd(n,γ) rates used in the stellar model calculations: the blue line corresponds to the cross section recommended by Bao et al. [10] and used also in the aforementioned works [2, 5]. The recent ASTRAL evaluation [11], shown in red, slightly improves the agreement with the SiC data, but is not sufficient to match them. In order to obtain the best fit to the experimental abundance ratios, an enhancement of 15% of the ^{146}Nd capture cross section value of ASTRAL (yellow line) is required.
In the right panel of Fig. 1 we present a summary of all the Nd isotope ratios predicted by the s-process calculations compared to the data of extrapolation of Richter's data [1] to ^{150}Nd=0 (i.e., δ_{Nd150}=-1000), which represents the pure s-process component. The

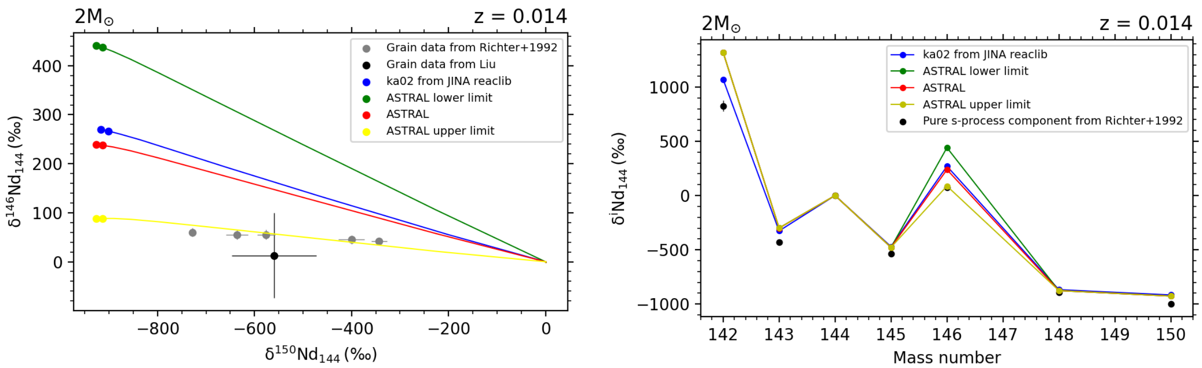

Figure 1: Left: δ-values (per mil deviations from solar system ratios) of ^{146}Nd/^{144}Nd relative to ^{150}Nd/^{144}Nd. AGB star calculations with different ^{146}Nd(n,γ) rates are compared with SiC grain data (see text for details). Dots along the curves represent third dredge-ups (TDUs) in the C-rich phase where SiC grains can form. Right: Nd-isotopic s-process abundance ratios normalized to ^{144}Nd. The extrapolated pure s-process value from the experimental data of [1] is compared to the same model calculations as in the left panel.

models are generally higher than the data, which may reflect an underestimation of the ^{144}Nd production, with the ^{146}Nd/^{144}Nd ratio showing the largest discrepancy. These are removed when using a model calculation with an enhancement of 15% of the ^{146}Nd capture cross section.

Although the ^{146}Nd(n,γ) cross section was varied in this sensitivity study over the whole energy range, a change of the rate in the low energy range ($\leq$20 keV) only produces, according to the calculations, a similar result (see complementary material [24]). This means, that the MACS at 30 keV may not need to be mostly modified and points to the relevance of the cross section at kT=8 keV. This value is largely influenced by the resonance region, never measured before.

The aforementioned stellar model calculations used as a reference the ^{146}Nd(n,γ) cross section of Bao et al. [10], which is based on the accurate time-of-flight (TOF) data provided by Wisshak et al. [12]. This data set, which covers the cross section in the unresolved resonance region (URR) from 3 to 225 keV, is also followed by all the evaluations, as shown in Fig. 2.

However, other existing measurements show large discrepancies with the data of Wissak, many of them reporting a significantly higher cross section. A compilation of such existing measurements can be found in [13]. Moreover, none of the existing data sets found in EXFOR [14] covers the resolved resonance region (RRR), which extends from 300 eV up to around 10 keV and, as a consequence, has a major impact in the capture rate at low stellar temperatures, the most relevant for the prediction of the ^{146}Nd/^{144}Nd ratio according to the aforementioned calculations.

With the aim of solving the present discrepancies in the ^{146}Nd(n,γ) cross section in the keV range (see Fig. 2) and matching the stellar models to the stardust observations, we propose a new measurement of this cross section at the CERN n_TOF Facility. Combining the high-flux facility n_TOF-EAR2, a high sensitivity setup, and the use of a high-purity sample of ^{146}Nd, we aim to measure for the first time the resonance region, thus allowing a

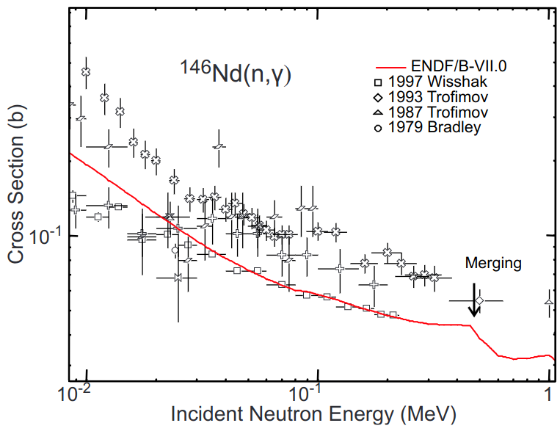

Figure 2: Evaluated capture cross section of ^{146}Nd (ENDF/B-VII.0 = ENDF/B-VIII.0 = JEFF-3.3) in the URR compared to the existing measurements. Figure from Ref. [13]

consistent re-evaluation of the cross section, focused mainly in the low stellar temperature range kT=8 keV. The details of the experimental setup are described in Sec. 2. Sec. 3 presents the feasibility study, the justification of the proton request, and the expected results.

2 Experimental setup and sample

High quality samples with sufficient mass and purity are key for the success of a neutron capture TOF experiment. This is particularly critical for samples of elements with many stable isotopes, such as Nd. For this experiment, we have obtained 80 mg of Nd oxide, containing 98.74% of ^{146}Nd and less than 0.5% of any other Nd isotope. One of the key aspects of these material is the absence (less than 0.1%) of ^{143}Nd, which has a very large (n,γ) cross section. The full isotopic composition of the sample is ^{142}Nd : ^{143}Nd : ^{144}Nd : ^{145}Nd : ^{146}Nd : ^{148}Nd : ^{150}Nd : 0.17 : $\leq$0.1: 0.4 : 0.21 : 98.74 : 0.32 : 0.1. The material, in the form of powder, will be encapsulated in a thin aluminium or PEEK capsule, making a sample of 10 mm in diameter.
Concerning the choice of experimental area, given the relatively small amount of material (80 mg), n_TOF-EAR2, featuring the largest instantaneous neutron flux worldwide, is the best solution to achieve good statistics. Moreover, the installation of the third generation spallation target during LS2 has lead to a remarkable improvement in energy resolution in EAR2 [15], a key factor for both increasing the signal-to-background ratio (SBR) and obtaining accurate resonance parameters. As shown in Sec. 3, the improved resolution will allow to resolve individual resonances of ^{146}Nd(n,γ) up to 5 keV.
To sustain the high counting rates associated to the instantaneous flux of n_TOF-EAR2, the new array of segmented C_6D_6 detectors, so-called s-TED [16], will be used in this measurement. In order to optimize the signal-to-background ratio of the setup, the array will be arranged in a compact-ring configuration [17] around the capture sample, as shown in the left panel of Fig. 3. This setup was already successfully used for two challenging (n,γ) measurements on the unstable ^{94}Nb [17] and ^{79}Se [18].

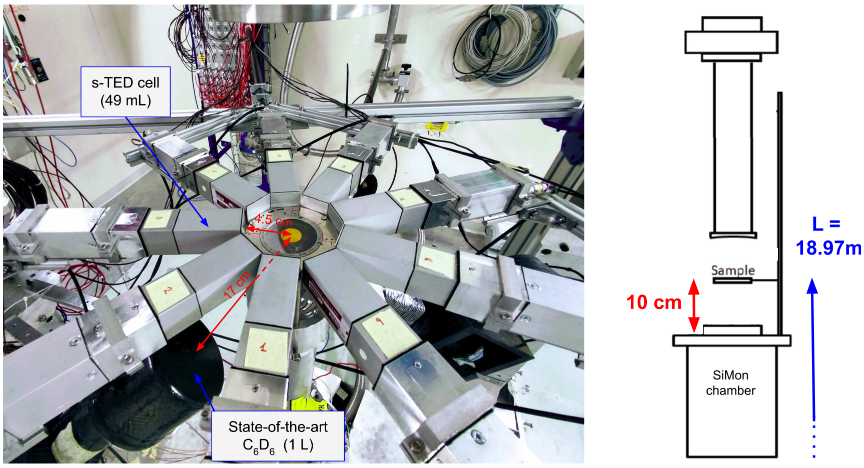

Figure 3: Photograph of the s-TED detector cells in the innovative ring configuration used in EAR2 that allows to place them at only 4.5 cm from the sample (left). Sketch of the optimum height of the capture sample (and detectors) in EAR2 (right).

In the last year, the performance of this setup was further optimized after a set of systematic studies with the aim of enhancing the sensitivity and increasing the efficiency for future neutron capture experiments at n_TOF-EAR2 [19]. Following the results of this campaign, we will place the plane of sTED detectors aligned with the sample at a height of only 10 cm above the SiMon chamber corresponding to a flight path of 18.97 m (see right panel of Fig. 3). With this modification, we will gain 60% in beam interception factor and 70% in total signal-to-background ratio with respect to the setup used in previous years.

3 Counting rate estimates, feasibility and expected results

The counting rate estimates have been calculated using the flux of n_TOF EAR2 extracted from Monte-Carlo (MC) simulations and validated with the preliminary experimental results [20]. The capture cross sections of all the Nd isotopes contained in the sample were obtained from the JEFF-3.3 evaluation. The (n,γ) efficiency of the full s-TED ring of approximately 4.5% was calculated by comparing the experimental results to the count rate predictions for ^{197}Au(n,γ) [24]. The beam-related background of EAR2 has been taken from experimental data measured with the same setup [15]. The fraction of the beam intercepted by the sample, equal to 0.26, was obtained from MC simulations combined with the recent gain factor determined in the optimization campaign. Last, the Resolution Function was taken from the accurate MC simulations of the new spallation target [20, 18]. The resulting count rate per pulse for the ^{146}Nd sample is compared to that of the background in the left panel of Fig. 4, showing that most of the resonances will be above the level of the background, hence clearly observable.
Because of the high accuracy required to solve the present discrepancies we have included in this proposal a study to evaluate the feasibility of the experiment and the expected re-

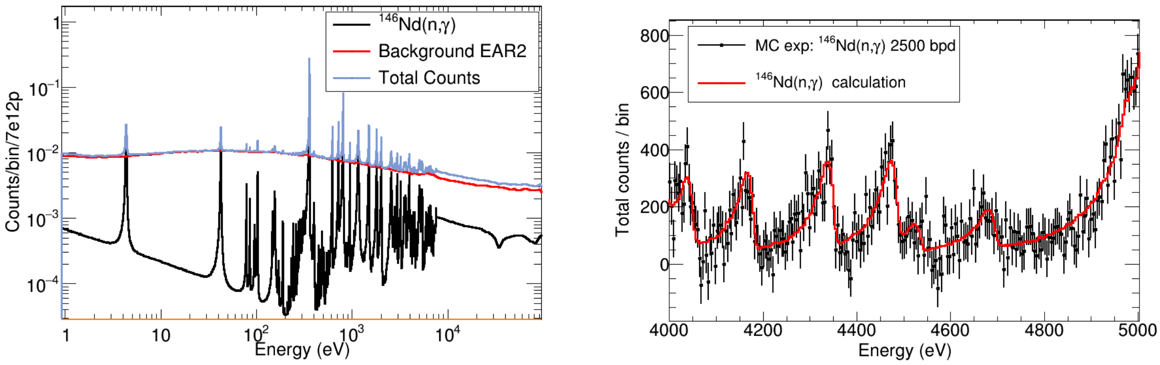

Figure 4: Right: Expected ^{146}Nd(n,γ) (+ contaminants) and background counts per pulse as a function of the neutron energy using the ring of s-TEDs in the optimum height. Left: results from the MC experiment showing the expected results with 2500 bins per decade (bpd) and the calculations in the upper energy range of the RRR.

sults. In the RRR, the number of observable resonances will depend on the statistics, the uncertainty associated with the background subtraction, and the broadening associated to the neutron energy resolution of the facility. To realistically simulate the statistical uncertainties we have implemented a MC resampling method and assigned a given number of protons to the sample (^{146}Nd and other Nd isotopes) and to the background measurements. The final number of protons considered for this MC experiment for each sample is listed in Table 1. The results indicate that, thanks to the improved resolution of EAR2 and the high flux, with the requested number of protons we will be able to observe and resolve most resonances up to 5 keV, as shown in the right panel of Fig. 4. This plot resembles the experimental capture yield, of which we will carry out the R-Matrix analysis ^{146}Nd capture cross sections using the SAMMY code [21]. Our estimates also indicate that the contamination from other Nd isotopes will be relevant only up to 300 eV, i.e., at energies lower than the first ^{146}Nd resonance. More details can be found in the complementary material. In order to assess the contribution of contaminants, a natural Nd sample of larger mass will be measured for a short period (see Table 1).

The number of observed resonances and the expected uncertainty in the extracted radiative kernels has been evaluated in terms of a statistical detection limit. The results of the detection limit study presented in Fig. 5 indicate that with the requested number of protons (Table 1) 23 out of the 28 resonances reported in the evaluations up to 5 keV will be observed (i.e., D$\leq$3 in the central panel) and analyzed with an uncertainty in the kernels below 10 % for most of them, as shown in the right panel of Fig. 5. More details can be found in the complementary material.

The final aim of the measurement is the determination of the stellar rates, especially the MACS at kT = 8 keV as well as at kT = 30 keV. Besides the direct impact of the measurement of the data in the RRR, the accurate measurement of the individual resonance parameters of 25 resonances (see Fig. 5) will be sufficient to provide a stringent constraint of the MACS in the relevant stellar energy range, following the same methodology based on the determination of the average resonance parameters used in previous measurements [22, 15]. Moreover, our estimates indicate that the proposed measurement may

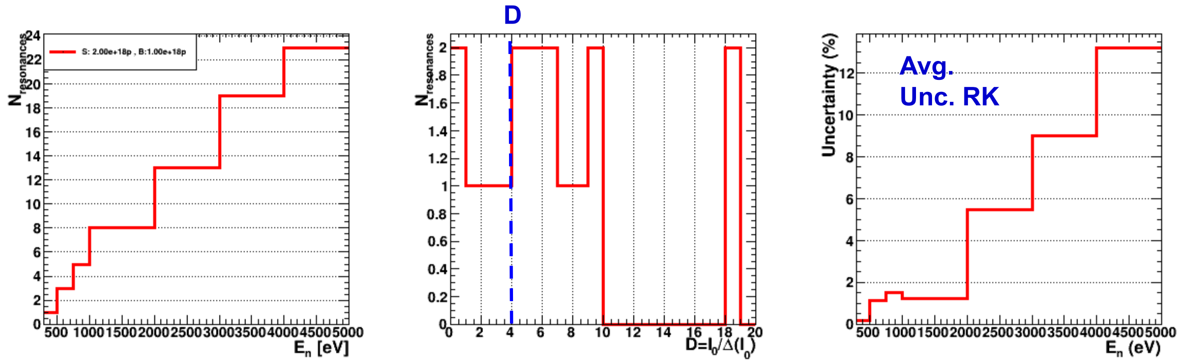

Figure 5: Cumulative number of observable resonances (left), distribution of resonances close to the detection threshold (center), and expected average uncertainty in the radiative kernel in different energy ranges (left).

be sensitive also to the cross section in the URR, with a signal-to-background $\simeq 0.2 : 0.8$, leading to a systematic uncertainty of roughly 5-7% associated to the background subtraction (see [24]).

Sample	Protons
^{146}Nd	2×10^{18}
^{nat}Nd	2×10^{17}
Dummy (background)	1×10^{18}
Au, C, Pb	5×10^{17}
Total	$\mathbf{3.7 \times 10^{18}}$

Table 1: Summary of the requested number of protons for the measurements in this proposal.

4 Summary and outlook

The measurement described in this proposal will help to solve the long-standing discrepancies in the ^{146}Nd abundance between stellar model calculations and stardust SiC data [5, 2] that may be solved with a 15% higher cross section.
For the preparation of this proposal we have carried out a realistic and conservative risk-assessment study, which shows the feasibility of the proposed experiment and the adequacy of the proposed setup, the choice of experimental area, and the beam-time request. The resulting data set will measure accurately the full resonance region up to at least 5 keV for the first time, and with larger systematic uncertainties also the URR. This proposed measurement will allow a consistent re-evaluation of the cross section in the astrophysical range of interest, in particular at low temperatures (kT = 8 keV).
As an outlook, we plan to complement this TOF measurement with a future proposal for an activation measurement at the new high-flux facility NEAR, which will serve to

access the MACS at various stellar temperatures following a methodology currently under validation [23]. The half-live of the (n,γ) product (^{147}Nd, 11.03 d) is very well suited for the long irradiation cycles currently accessible in that facility.
Summary of requested protons: 3.7×10^{18}.

References

[1] S. Richter et al., Abstracts of the Lunar and Planetary Science Conference, 23, page 1147, (1992)

[2] T. R. Ireland et al., Geochimica et Cosmochimica Acta 221, 200-218 (2018)

[3] E. Zinner, Astrophysical Journal Letters 382, p. 47 (1991)

[4] P. Hoppe and U. Ott, AIP Conf. Proc. 402, 27–58 (1997)

[5] Q.Z. Yin et al., The Astrophysical Journal, 647, 676–684 (2006)

[6] M. Lugaro, S. Cristallo et al. Private communication

[7] S. Cristallo et al., ApJS 219 40 (2015)

[8] A. I. Karakas and M. Lugaro, The Astrophysical Journal, 825, 262016 (2016)

[9] N. Liu, Isotopic compositions of s-process elements in acid-cleaned mainstream presolar silicon carbide. Ph.D. Thesis, University of Chicago, Chicago (2014)

[10] Z.Y. Bao, H. Beer, F. Käppeler, et al., Atomic Data Nucl. Data Tables 76, 70 (2000)

[11] R. Reifarth, et al., European Physical Journal Plus 133, 424 (2018)

[12] K. Wisshak et al., Phys. Rev. C 57, 391 (1998)

[13] H. I. Kim et al., Nuclear Science and Engineering, 160:2, 168-189 (2008)

[14] N. Otuka et al., . Nucl. Data Sheets 120, 272 (2014)`https://www-nds.iaea.org/exfor/`

[15] J. Lerendegui-Marco et al., EPJ Web of Conferences 284, 01028 (2023)

[16] V. Alcayne et al., EPJ Web of Conferences 284, 01043 (2023)

[17] J. Balibrea et al. et al., EPJ Web of Conferences 279, 06004 (2023)

[18] J. Lerendegui-Marco et al., EPJ Web of Conferences 279, 13001 (2023)

[19] J. Lerendegui-Marco, M. Bacak et al., CERN-INTC-2023-036 ; INTC-P-587-ADD-1 (2023)

[20] J. A. Pavón-Rodríguez et al., EPJ Web of Conferences 284, 06006 (2023)

[21] N. M. Larson, *Updated Users' Guide for SAMMY: Multilevel R-Matrix Fits to Neutron Data Using Bayes' Equations*, ORNL/TM 9179/R8 (2008).

[22] C. Guerrero et al., Phys. Rev. Lett. 125, 142701 (2020)

[23] E. Stamati et al., EPJ Web of Conferences 284, 06009 (2023)

[24] Complementary material

Appendix

DESCRIPTION OF THE PROPOSED EXPERIMENT

Please describe here below the main parts of your experimental set-up:

Part of the experiment	Design and manufacturing
If relevant, write here the name of the fixed installation you will be using: C6D6 (Legnaro and s-TEDs) present at the n_TOF installation	☒ To be used without any modification ☐ To be modified
If relevant, describe here the name of the flexible/transported equipment you will bring to CERN from your Institute: None	☐ Standard equipment supplied by a manufacturer ☐ CERN/collaboration responsible for the design and/or manufacturing

HAZARDS GENERATED BY THE EXPERIMENT

Additional hazard from flexible or transported equipment to the CERN site:

Domain	Hazards/Hazardous Activities		Description
Mechanical Safety	Pressure	☐	[pressure] [bar], [volume][l]
	Vacuum	☐	
	Machine tools	☐	
	Mechanical energy (moving parts)	☐	
	Hot/Cold surfaces	☐	
Cryogenic Safety	Cryogenic fluid	☐	[fluid] [m3]
Electrical Safety	Electrical equipment and installations	☐	[voltage] [V], [current] [A]
	High Voltage equipment	☐	[voltage] [V]
Chemical Safety	CMR (carcinogens, mutagens and toxic to reproduction)	☐	[fluid], [quantity]
	Toxic/Irritant	☐	[fluid], [quantity]
	Corrosive	☐	[fluid], [quantity]
	Oxidizing	☐	[fluid], [quantity]
	Flammable/Potentially explosive atmospheres	☐	[fluid], [quantity]
	Dangerous for the environment	☐	[fluid], [quantity]
Non-ionizing radiation Safety	Laser	☐	[laser], [class]
	UV light	☐	
	Magnetic field	☐	[magnetic field] [T]
Workplace	Excessive noise	☐	
	Working outside normal working hours	☐	
	Working at height (climbing platforms, etc.)	☐	

	Outdoor activities	☐	
Fire Safety	Ignition sources	☐	
	Combustible Materials	☐	
	Hot Work (e.g. welding, grinding)	☐	
Other hazards			